

EuroEcho-Imaging 2014: highlights

Julien Magne^{1,2*}, Gilbert Habib^{3,4}, Bernard Cosyns⁵, Erwan Donal⁶,
Owen Miller⁷, Danilo Neglia⁸, Steffen E. Petersen⁹, and Patrizio Lancellotti^{10,11}

¹CHU Limoges, Hôpital Dupuytren, Service Cardiologie, Limoges F-87042, France; ²Faculté de médecine de Limoges, INSERM 1094, 2, rue Marcland, 87000 Limoges, France; ³Department of Cardiology, Aix-Marseille Université, 13284 Marseille, France; ⁴La Timone Hospital, 13005 Marseille, France; ⁵UZ Brussel-CVHZ, 1090 Brussels, Belgium; ⁶CIC-IT U 804, CHU Rennes, Université Rennes 1, Service de Cardiologie, CHU RENNES, Rennes, France; ⁷Department of Congenital Heart Disease, Evelina London Children's Hospital, London, UK; ⁸Fondazione CNR/Regione Toscana G. Monasterio, Pisa, Italy; ⁹William Harvey Research Institute, NIHR Cardiovascular Biomedical Research Unit at Barts, Queen Mary University of London, London, UK; ¹⁰Department of Cardiology, Heart Valve Clinic, CHU Sart Tilman, University of Liège Hospital, GIGA Cardiovascular Sciences, Liège, Belgium; and ¹¹GVM Care and Research, E.S. Health Science Foundation, Lugo, Ravenna, Italy

Received 16 March 2015; accepted after revision 16 March 2015; online publish-ahead-of-print 28 April 2015

The annual meeting of the European Association of Echocardiography (EuroEcho-Imaging) was held in Vienna, Austria. In the present paper, we present a summary of the 'Highlights' session.

Keywords heart failure • heart valve disease • 3D echocardiography • cardiac magnetic resonance • congenital heart disease • nuclear cardiology • cardiac computed tomography

Introduction

The third annual scientific meeting of the European Association of Cardiovascular Imaging (EACVI), EuroEcho-Imaging 2014, was held in Vienna, Austria. The main themes were 3-dimensional imaging and imaging in acute cardiac care. The meeting was a great success with a record number of participants (>3500 delegates) and over 1300 abstracts submitted. The last day of the meeting, the 'Highlights' session wrapped up the event with a summary of the most relevant abstracts presented throughout the congress. A short report of this session is presented below.

Heart failure

Patients with non-ischaemic cardiomyopathy are better responders to cardiac resynchronization therapy (CRT) than those with ischaemic cardiomyopathy. It was therefore relevant to identify echocardiographic predictors of ischaemic and non-ischaemic left bundle branch block (LBBB). Using 2-dimensional speckle tracking echocardiography (2D-STE) analysis, Baum *et al.* have investigated displacement, transversal, and longitudinal strains. Only longitudinal strain was accurate to distinguish ischaemic from non-ischaemic LBBB.¹ The comparison of peak basal longitudinal systolic strain between septal and posterolateral wall helped to distinguish LBBB with or without coronary artery disease.

Mechanical dyssynchrony may be assessed visually. Szulik *et al.* have underlined the value of visual assessment of left ventricular (LV) apical rocking. Nevertheless, visual assessment is difficult to

standardize,² and in this regard, they identified two new quantitative tools based on 2D-STE techniques: (i) the early systolic peak longitudinal strain/global longitudinal strain ratio, and (ii) the positive/negative ratio of peak left regional displacement at end-systole (a parametric imaging is generated and displayed in *Figure 1*). These two approaches measure the amount of septal flash and LV apical rocking. Regarding the prediction of LV reverse remodelling at 6-month post CRT, these two parameters showed similar accuracy (area under the curve ~ 0.85) and reproducibility (intra-class correlation coefficient for intra- and inter-observer variability ~ 0.9)³ (*Figure 1*).

Hasselberg *et al.*⁴ have assessed at the mechanical consequences of CRT and their relationships with LV reverse remodelling. They found that remodelling process was more related to improvement of LV longitudinal than circumferential function.

Cardiotoxicity is a leading cause of morbidity and mortality in cancer survivors. Early detection could improve the management and prognosis in these patients. Blazquez Bermejo *et al.*⁵ performed echocardiography before and regularly after a treatment by chemotherapy (alkylating agents and anthracyclines ~90%, radiotherapy ~ 1/3 of the wall population). They demonstrated a decrease in LV global longitudinal strain (GLS) ~15% at 3-month follow-up echocardiography in patients who developed cardiotoxicity (i.e. defined as Cardiotoxicity diagnosis: LVEF decrease >10% and below 55% at 12 months; 11% of patients studied). By opposition, there was no change in LV longitudinal function in patients without cardiotoxicity. These results support the systematic use of GLS in these patients.

In a large cohort of hypertrophic cardiomyopathy ($n = 472$) explored with a median follow-up of 4.4 years, Reant *et al.*⁶ have

* Corresponding author. Tel: +33 62 40 42 361; Fax: +33 55 50 56 334, E-mail: jul.magne@yahoo.fr

Published on behalf of the European Society of Cardiology. All rights reserved. © The Author 2015. For permissions please email: journals.permissions@oup.com.

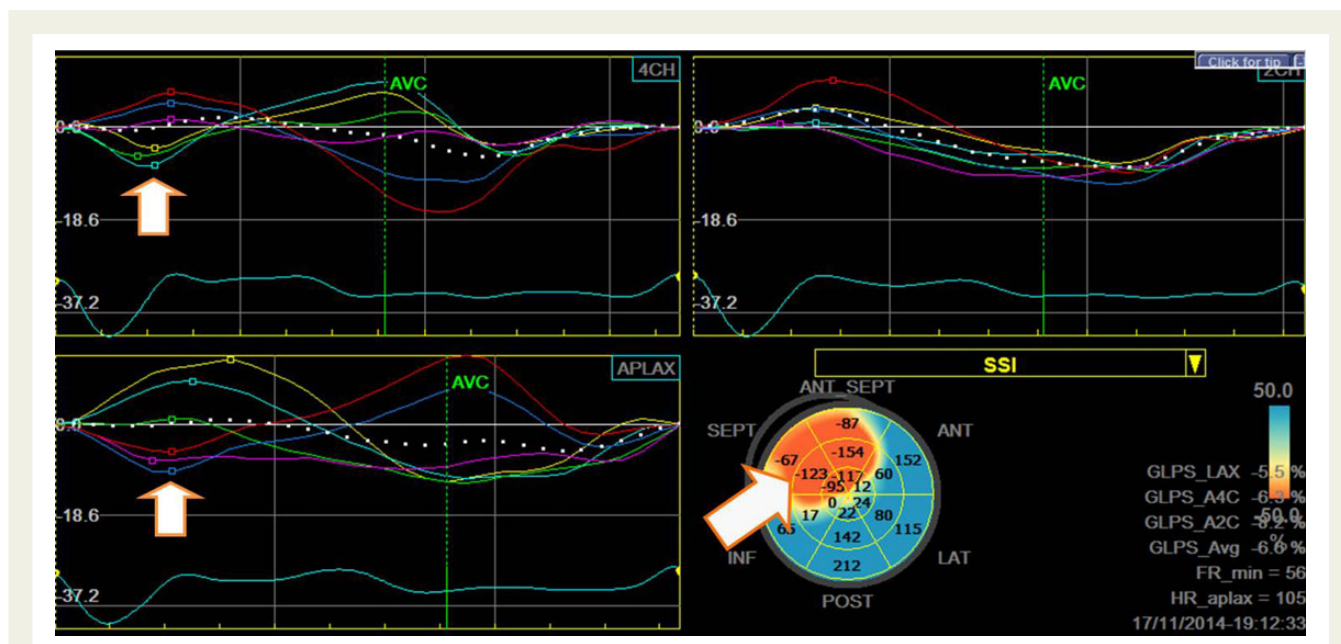


Figure 1 New quantitative approach based on longitudinal assessment of strain: detection of both negative and positive strain peaks in first half of systole. Start systolic index (%) = integrates peak strain values and global strain values; Color map: Red (contraction); Blue (stretching).

demonstrated that a previous history of non-sustained ventricular tachycardia, NYHA functional class III-IV, LV end-systolic volume, $GLS \leq 14\%$, and resting LV outflow tract gradient ≥ 30 mmHg were independent predictors of cardiovascular death or appropriate implantable cardioverter defibrillator therapy.

Recent data in cardiac amyloidosis (CA) have encouraged the use of LV longitudinal strain. Ternacle et al.⁷ have reported the lack of difference in late gadolinium enhancement (LGE) according to CA aetiologies. However, they found an inverse relationship between the degree of alteration of LV longitudinal strain and the amount of fibrosis, as estimated by LGE. An apical longitudinal strain greater than -14.5% was an independent prognostic marker, regardless CA aetiologies.

Valvular heart disease

The major role of multi-imaging modalities in the assessment, management, and risk stratification of patients with valvular heart disease continues to grow up. This year again, the large majority of selected abstracts in the field of valvular heart disease explored aortic stenosis (AS). In this regard, Saura et al.⁸ measured using real-time 3D transoesophageal (TOE) echocardiography the planimetry of aortic valve area in 282 AS patients. They reported that this parameter was independently associated with significant reduced survival and that 0.8 cm^2 (and not 1 cm^2) was the most appropriate cut-off to predict mortality.

Following transcatheter aortic valve implantation, Scherzer et al.⁹ reported the serial pre- and post-intervention (i.e. at 30-day, 6-month, and 1-year follow-up) Nt-pro BNP level of 142 patients. They found a progressive and significant decrease in the biomarker level and that both baseline (i.e. pre-intervention) and serial

changes in Nt-pro BNP [Hazard ratio (HR) = 1.34, $P = 0.012$ and HR = 1.58, $P = 0.0002$, respectively] were associated with reduced mid-term survival.

Kramer et al.¹⁰ have elegantly studied 77 patients with serial echocardiographies showing evolution from non-severe AS to diagnosis of severe AS (aortic valve area $< 1 \text{ cm}^2$). Subsequently, the patients were studied according to mean transvalvular pressure gradient (i.e. \geq or < 40 mmHg), and patients with low gradient were subcategorized according to indexed stroke volume (i.e. \geq or $< 35 \text{ mL/m}^2$). Patients with high gradient ($n = 31$) depicted faster progression of AS from baseline to follow-up, with significant greater decrease in aortic valve area ($P = 0.044$) and increase in peak aortic velocity ($P < 0.001$), compared with patients low flow-low gradient AS ($n = 28$). In contrast, patients with low flow-low gradient showed the worst LV myocardial longitudinal impairment and, as a result, significantly worst functional deterioration and lower mid-term survival ($P = 0.021$).

In two separately analysed studies including symptomatic patients with severe AS and preserved LV ejection fraction, Galli et al.^{11,12} aimed to investigate the prognosis significance of both reduced RV function, as assessed using TAPSE, and reduced LA longitudinal function (Figure 2). In a cohort of 201 patients, they have first demonstrated a significant impact of reduced TAPSE (i.e. ≤ 17 mm) on overall mortality ($P = 0.03$). Similarly, they secondly ($n = 178$) identified that peak LA strain $\leq 23\%$ was significantly associated with increased risk of 2-year occurrence of major adverse cardiovascular event ($P = 0.03$) and with trend to higher mortality ($P = 0.05$).

In a tremendous study including patients with heart failure and reduced LV ejection fraction, Bandera et al.¹³ simultaneously performed stress exercise echocardiography combined with cardiopulmonary exercise test including gas exchange analysis. They classified

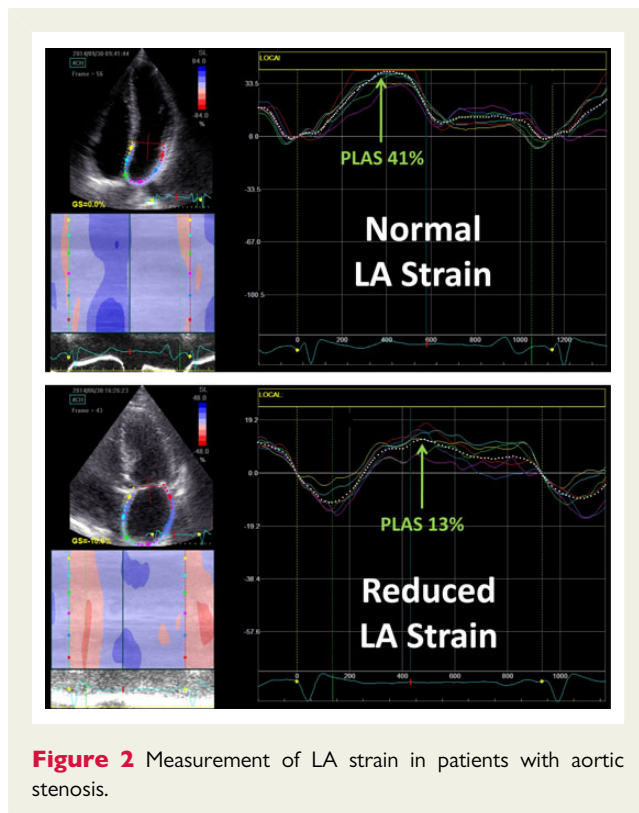


Figure 2 Measurement of LA strain in patients with aortic stenosis.

their patients according to resting and exercise MR severity [Group A: both resting and exercise effective regurgitant orifice area (EROA) $< 20 \text{ mm}^2$, $n = 60$; Group B: resting EROA $< 20 \text{ mm}^2$ but exercise EROA $> 20 \text{ mm}^2$, $n = 17$; Group C: both resting and exercise EROA $> 20 \text{ mm}^2$, $n = 25$). They found that patients in the Group B (i.e. those with dynamic MR) had functional limitation similar to patients with resting severe MR, mainly characterized by development of exercise pulmonary hypertension. In addition, patients with resting severe MR depicted the worst profile in term of bi-ventricular remodelling, lack of contractile reserve, and impaired ventilatory function, and those without exercise severe MR had the best functional status and outcome. Furthermore, patients in Group B seem have intermediate outcome compared with the two other groups.

Finally, the functional and prognosis significance of left-sided valvular thickening (LVT) was tested in 150 patients with systemic light-chain amyloidosis by Pradel *et al.*¹⁴ They have found that patients with LVT (42%), as visually assessed using echocardiography, more frequently have Mayo clinic stage III and NYHA functional class \geq III than those without LVT. Consistently, they reported a significant lower overall survival at 2- and 6-year follow-up.

3-Dimensionnal echocardiography

3D echocardiography is a fascinating and emerging technology for imaging the heart. Real-time full-volume 3D echocardiography (3DE) allows rapid and non-invasive measurement of left (LA) and right atrial (RA) volume without making geometric assumptions. Different softwares with semiautomatic endocardial contour finding

algorithms from different commercial providers are available. Mueller *et al.*¹⁵ have compared LA and RA volume determined by these algorithms. They found an excellent linear correlation and agreement for both LA and RA between volumes determined by EchoPAC and QLAB software, respectively, indicating that values of LA and RA atrial volume obtained by either algorithm can be compared, for example during follow-up examinations.

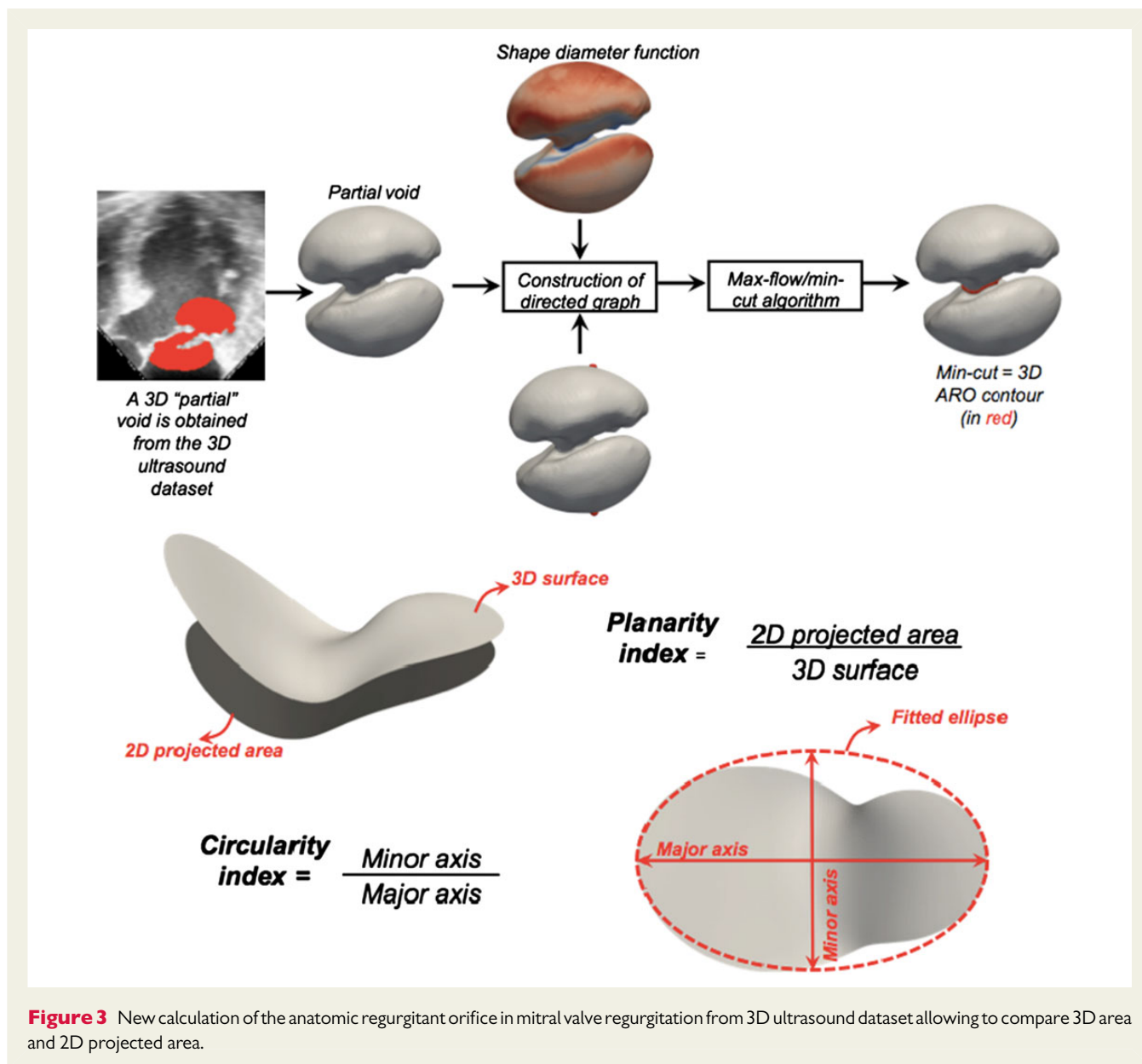
Luo *et al.*¹⁶ have studied 82 consecutive bradycardia patients requiring right ventricular (RV) pacing with dual-chamber devices. They have performed 3DE before and 12 months after RV pacing to determine the effect on LV volumes, mass, and LV global deformation. They observed an increase in LV volumes and mass, a reduction in LV ejection fraction and a significant reduction in global strain (longitudinal, radial, and circumferential).

In a study from Dreyfus *et al.*,¹⁷ TOE 3D dynamic volumetric data of the tricuspid annulus (TA) were acquired in 184 patients. Long- and short-axis diameters and the area of the TA at the time of its maximal opening were measured. The eccentricity index (EI) of the TA was defined as long-axis/short-axis ratio and TA orientation as the angle between the interatrial septum axis (aortic valve on the top at 0°) and the long-axis in the surgical view. 3D-TOE allowed a good assessment of the TA shape and orientation, which is significantly different among individuals. TA dilatation occurred homogeneously in all the directions of the RV free wall as attested by the very good correlation between the TA area and both long axis ($r = 0.89$, $P < 0.0001$) and short axis ($r = 0.88$, $P < 0.0001$). TA dilatation, as shown by increase in TA area, was associated with a small decrease of EI, thus a trend to a more circular TA. All orientations of TA were observed, from 5° to 175° (mean = $87^\circ \pm 57^\circ$) with a bimodal distribution (most frequently at 40° and 150°).

Sotaquira *et al.*¹⁸ have developed a semi-automated method for 3D area of regurgitant orifice (ARO) quantification from TOE images (Figure 3) and validated it against manual planimetry in 25 patients with mild to severe mitral regurgitation (MR). On the systolic frame, an initial supervised segmentation of the region including the ARO was performed, followed by an automated graph-based extraction of ARO 3D contour, from which 3D surface and 2D projected areas, circularity (CI) and planarity (PI) indices were computed. The proposed semi-automated method resulted in accurate detection of ARO compared with manual planimetry. 3D ARO assessment showed underestimation of 2D measures, together with generally non-circular and non-planar orifices, highlighting the limitations of current clinical approach in the assessment of MR severity.

Miglioranza *et al.*¹⁹ compared the role of 2DE diameters and 3DE TA surface area (TASA) to predict the severity of functional tricuspid regurgitation (FTR) in a prospective cross-sectional study of 24 patients. In comparison with 2DE TA diameters, TASA showed better correlations ($P < 0.0001$) with 3D parameters of FTR severity. Considering the FTR severity as the outcome, receiver operative characteristic (ROC) curve analysis revealed that TASA has a greater predictive power to discriminate severe from non-severe FTR [area under curve (AUC) = 0.84] than 2DE TA diameters measured in four-chamber (AUC = 0.63) or parasternal long-axis view (AUC = 0.51).

A study from Meyer *et al.*²⁰ sought to evaluate regional LV function after transfemoral (TF) and transapical (TA)-TAVI by 3D-STE compared with Cardiac Magnetic Resonance feature tracking (CMR - FT) analysis performed 3 months after TAVI in 36 consecutive



patients (18 TA- and 18 TF-TAVI) without atrial fibrillation or prior myocardial infarction. While CMR strain analysis detects apical LV dysfunction after TA-TAVI, 3D-STE was less sensitive in the detection of the apical function defect.

Real-time 3D contrast TOE has potential advantage for the diagnosis of small patent foramen ovale (PFO). It also allows direct visualization of the entire fossa ovalis and surrounding structures. It results in more accurate diagnosis of PFO by directly visualizing the bubbles crossing the fossa ovalis. Rotzak et al.²¹ performed RT3D contrast TOE in 121 consecutive patients referred for stroke. The diagnosis of PFO was obtained in 25 patients. In three of them, the bubbles were visualized only on RT3D. High-quality 3D images suggested that 3DTEE is feasible and provided detailed description of the atrial septum anatomy and PFO anatomy.

Goebel et al.²² assessed LA appendage (LAA) dimensions comparing 2D- with 3D-TOE measurements before, during, and 45 days

after intervention in 74 patients undergoing percutaneous LAA occlusion by the Watchman[®] device. Compared with 3D-TOE, 2D-TOE significantly underestimates maximal LAA orifice diameter and is associated with higher observer variability and lower reliability. Finally, comparing the EI, device implantation leads to a change of LAA orifice shape and dimensions.

CMR Imaging

CMR images contain an abundance of quantifiable information. Analysis approaches are mostly manual and thus time consuming. CMR LGE images have been shown to be accurately quantified using a fully automated 3D LV myocardial scar detection using a Gaussian mixture model compared with the manual gold standard (Figure 4).²³

An elegant experimental model used CMR to study cardiotoxic effects. Authors demonstrated that the encapsulation of doxorubicin

with liposome resulted in less adverse cardiac remodelling (LV ejection fraction, RV ejection fraction, and prevalence of myocardial fibrosis) compared with standard doxorubicin.²⁴

Incidental non-cardiac findings are not rare. In 5135 CMR studies from three centres, the overall prevalence was 6.1%. Severe findings were found in 1.6% of CMR studies. The severe findings were more common in men and in those undergoing stress CMR, possibly related to higher prevalence of shared risk factors (e.g. smoking) for other pathologies.²⁵

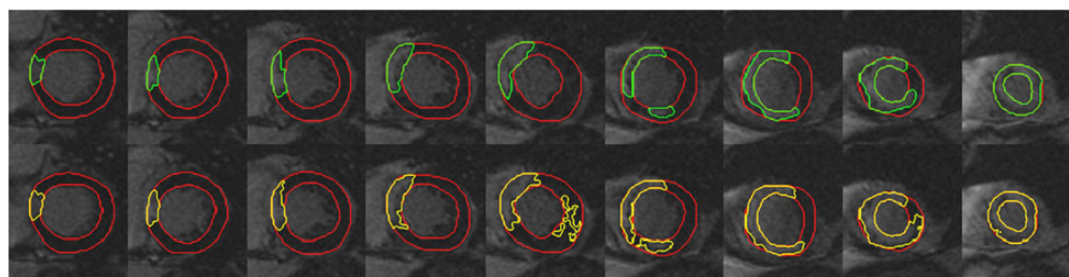
In patients with severe primary MR with hearts of normal size and function, 29% showed LV remodelling and LV impairment 6 months after mitral valve surgery. LGE was associated with post-operative impairment (80% with post-op LVEF < 50% showed LGE compared with 23% if LVEF > 50%, $P = 0.047$).²⁶

Suspected inflammatory pericarditis benefits from a comprehensive CMR approach assessing pericardial and cardiac morphology including tissue characterization. In addition, a positive relationship between the degree of pericardial thickening and other parameters of inflammation was observed.²⁷

In a randomized trial comparing the value of cardiac CT and CMR approaches to assess the LA and pulmonary veins prior to radio-frequency ablation in patients with drug refractory paroxysmal or persistent atrial fibrillation (AF) LA volume measured by CMR remained the only robust independent predictor of AF recurrence. A lower overall cumulative radiation was observed despite similar outcomes for CMR-guided compared with CT-guided AF ablations (32.8 ± 23.5 vs. 40.4 ± 23.7 mSv, $P < 0.005$).²⁸

The LA volumes determined by CMR can predict AF and adverse events in hypertrophic cardiomyopathy, whereas prevalence of myocardial fibrosis cannot. This interesting finding was presented based on retrospective data from 352 patients across five centres with a mean follow-up of 41 ± 24 months.²⁹

The differentiation of physiological from pathological LV hypertrophy can be challenging. A CMR study with male professional athletes ($n = 75$), male hypertrophic cardiomyopathy ($n = 92$), and male sedentary healthy volunteers showed that despite similar LV mass indexes for athletes and hypertrophic cardiomyopathy patients, a number of geometric indices combining regional hypertrophy and



Bland-Altman analysis

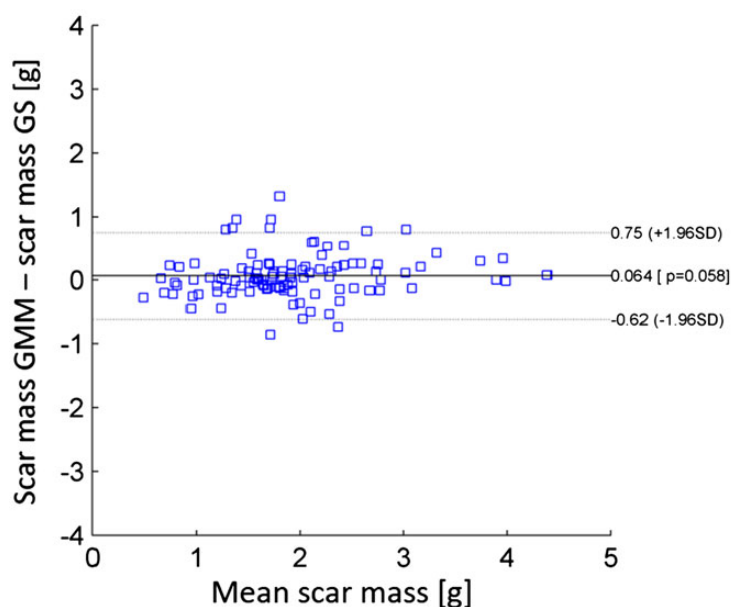


Figure 4 Top panel, first row shows short-axis LGE images with manual contouring of the area of myocardial infarction as the gold standard (GS). Top panel, second row displays the area of infarction identified using the Gaussian mixture model (GMM). Bottom panel shows in a Bland–Altman graph the minimal systemic bias and the excellent 95% agreement between the two methods.

LV size allowed reliable distinction between the two forms of LV hypertrophy.³⁰

A CMR study ($n = 94$, median 61-month follow-up) was presented and aimed to identify whether delayed revascularization in patients with ischaemic heart failure and evidence of viability was associated with improved survival compared with medical therapy alone. Patients with significant viability and ischaemic heart failure with NYHA III-IV derived most benefit from delayed revascularization. Patients with no viability, or with evidence of viability and NYHA I-II did not show improved survival following revascularization compared with optimal medical therapy.³¹

Increased pulmonary vascular resistance (PVR) estimated by CMR in systolic heart failure ($n = 105$, LVEF < 40%, prior heart failure admission) irrespective of aetiology and the presence of LGE predicted heart failure readmissions and all-cause mortality.³²

Many post-infarct patients with an indication for an implantable cardioverter defibrillator will not develop ventricular tachycardia. Measuring intramural scar surface and sub-epicardial scar surface by CMR appear promising tools to stratify the risk of post-infarct ventricular tachycardia.³³

Congenital heart disease

The Congenital Heart Disease (CHD) programme saw several major themes emerge in the abstract sessions. Multimodality imaging that finds a natural home in CHD was represented across several key themes predominantly Tetralogy of Fallot (TOF).

Timoteo et al.³⁴ presented data from a study aiming to identify whether RV and/or RA strains derived from 2D-STE are associated with arrhythmic events in patients with repaired TOF. Conventional parameters assessing RV function did not materially differ between patients with and without significant arrhythmia apart from the TA A'-wave velocity. However, when using 2DSTE, there was a significant difference in both the RV and RA strains parameters between arrhythmic and non-arrhythmic patients. Despite some study limitations, they concluded that compared with conventional echocardiographic parameters, 2DSTE strain measurements (particularly RV) are associated with arrhythmic events and that RV 2D strain may be useful for risk stratification of repaired TOF.

Staying with the RV, West et al.³⁵ evaluated the role of echocardiography vs. angiography in the developing field of Melody percutaneous pulmonary valve (MPPV) implantation. In 45 adult patients with CHD, they estimated the maximal instantaneous and mean Doppler gradient (ΔP_{max} and ΔP_{mean}) and degree of regurgitation as determined by conventional colour Doppler parameters. These data were compared with invasive post-implantation peak-to-peak gradient (ΔP_{p-p}) which had been recorded during the implantation procedure. The narrowest dimensions of the MPPV system were taken retrospectively from the final biplane orthogonal fluoroscopic images to calculate the effective valve orifice area (EOA). There was poor agreement between the invasive ΔP_{p-p} (11.5 ± 5.2 mmHg) and the ΔP_{max} and ΔP_{mean} (33.3 ± 8.2 mmHg and 19.3 ± 6.5 mmHg, respectively) with Doppler echocardiography being greater than the invasive pressures. There were only weak relationships between the indexed EOA and the invasive and Doppler gradients. They conclude that Doppler gradient for the percutaneous Melody valve system early after implantation is consistently higher than the invasive

ΔP_{p-p} gradient, but still provides a valuable baseline assessment for future serial assessment. These results reflect the complex and variable anatomy of the RV outflow tract/main pulmonary artery in this group of patients, all of whom had previously undergone surgery.

Moving on to new techniques, Kutty et al.³⁶ presented preliminary work on rotation intensity and energy dissipation of RV flow in TOF compared with normal controls using echo contrast Particle Imaging Velocimetry (PIV), which combines 2DSTE and contrast enhanced echocardiography to determine the velocity and direction of fluid streams by analysing the change in position of particles (Figure 5). Although previously described in LV, this study look more specifically at

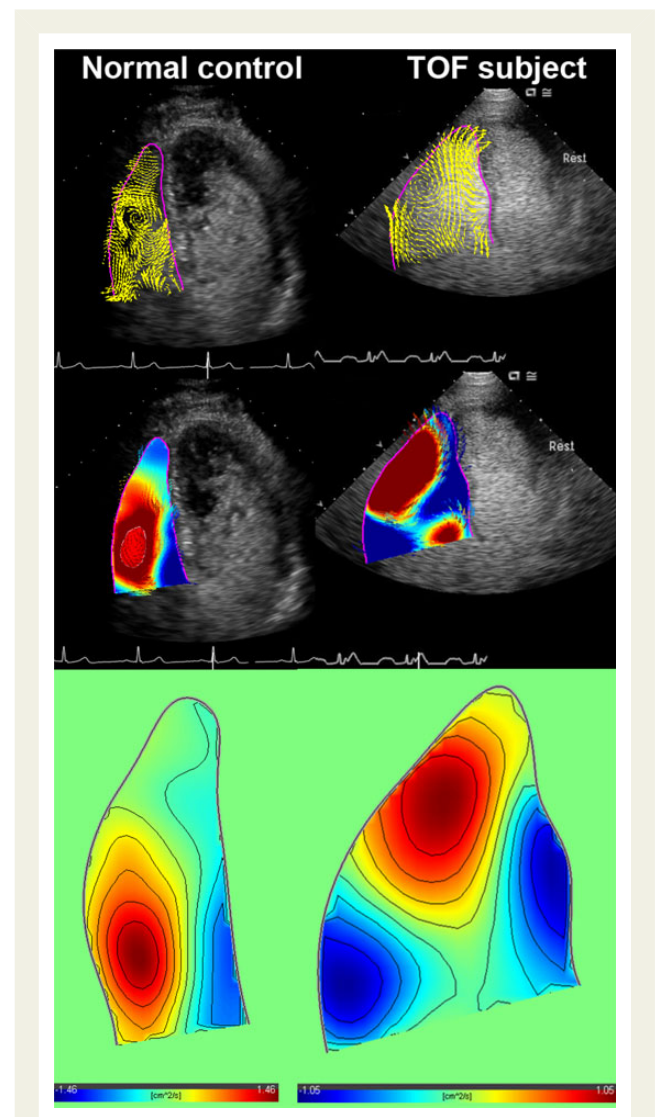


Figure 5 Echocardiographic particle imaging velocimetry derived RV flow field in a normal control (left panel) and in a patient with TOF (right panel). Each panel shows one image of the velocity vector field at one instant (upper), one colour map image of the rotation level at another instant with superimposed velocities (middle), and the colour map image of the rotation level for the steady-streaming (heartbeat averaged) flow field (lower panel). Red indicates counter-clockwise rotation, and blue indicates clockwise rotation.

the RV in 16 patients (13–42 years, median 22 years) with repaired TOF compared with 25 normal controls (23–43 years, median 34 years). Kinetic energy dissipation measure of amount of energy loss by friction, where the lower the energy dissipation in blood flow through the ventricular chamber, the higher the ventricular efficiency and flow rotation intensity was defined as the amount of swirl calculated 'inside the vortex' normalized with the total swirl in the whole chamber. The study was limited by the complex geometry of the RV, the two-dimensional nature of the technique and the difficulty in capturing progression of flow into the RV outflow tract in the four-chamber plane, the patients were not age matched and the number of patients was small. Despite these limitations, the investigators concluded that measurement of intraventricular flow parameters by PIV is feasible in both ventricles for normal individuals and most patients after surgical repair of TOF and that in this group of patients with repaired TOF and relatively favourable haemodynamic outcomes with preserved systolic function, RV, and LV flow parameters were different from those of normal controls.

The 3DE is now standard of care for CHD. Karsenty *et al.*³⁷ presented data from their study using 3D-TTE to assess ventricular septal defect (VSD) anatomy and severity. There were significant differences in the

maximum and minimum VSD diameters when measured on 3DE compared with 2D-TTE. The study conclusions were that 2D underestimates the VSD size compared with 3D and that 3D-TTE was useful to estimate VSD severity in some situations when the Doppler unhelpful.

Finally, Cantinotti *et al.*³⁸ presented initial data from a very large single-centre study of 1091 children (0–17 years) where 23 individual cardiac structures were measured echocardiographically to develop standardized nomograms for chamber dimensions and areas in paediatric echocardiography. This work represents the largest normal values report for healthy infants and children and will allow more accurate calculation of z score across the paediatric population.

Nuclear cardiology and cardiac computed tomography

Coronary CT angiography (CCTA) is an emerging imaging approach for the diagnosis of coronary artery disease (CAD). It is recommended by current ESC guidelines, as an alternative to other imaging modalities, in patients with stable chest pain and low-to-intermediate pre-test disease probability (PTP).

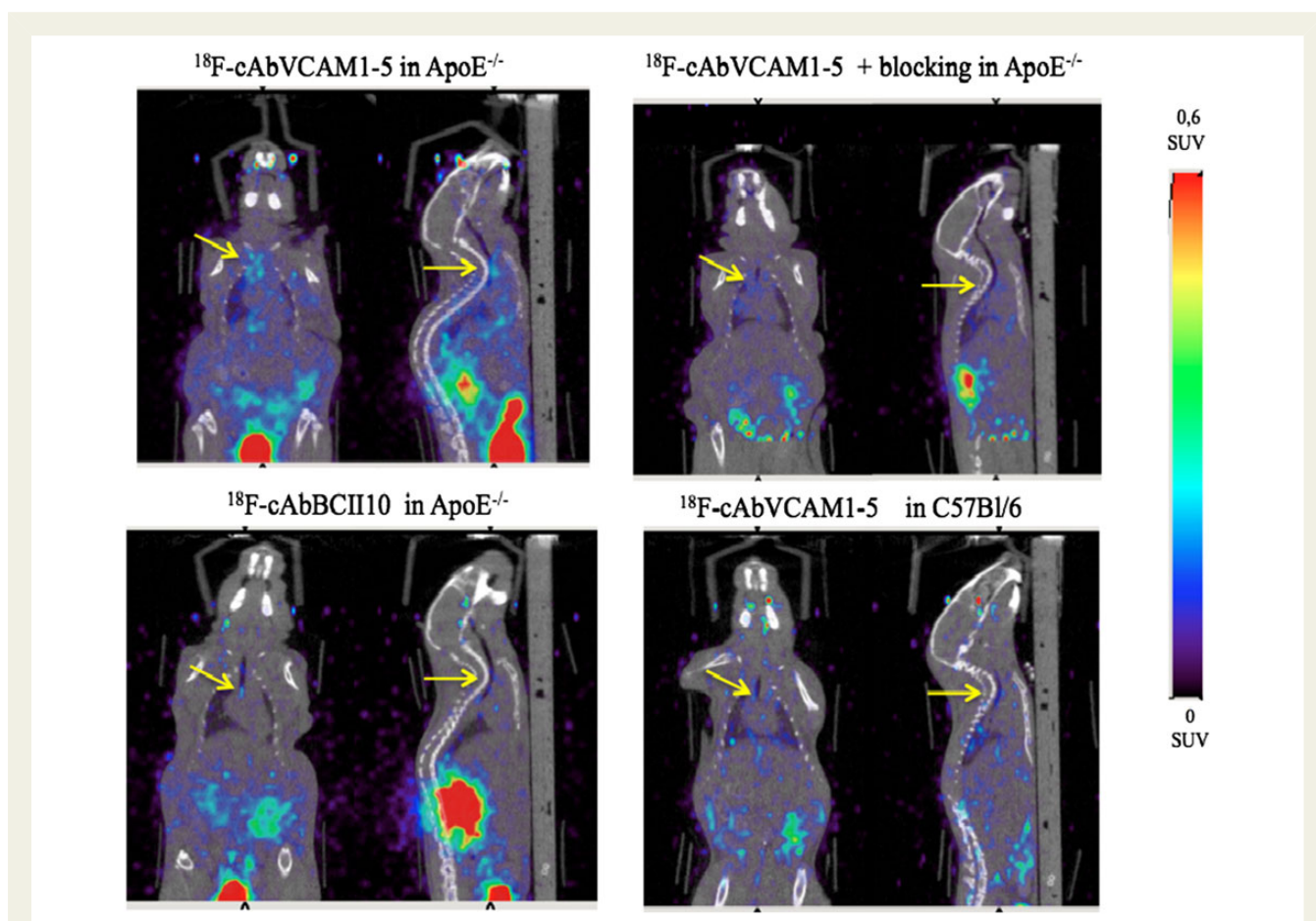


Figure 6 PET/CT imaging in ApoE^{-/-} and C57Bl/6 mice. Representative PET/CT images of ApoE^{-/-} and C57Bl/6 mice 2–3 h after injection of the radiotracer. Focal uptake of 18F-cAbVCAM1-5 nanobody is visible at the level of aortic arch of ApoE^{-/-} mice while background uptake is observed in C57Bl/6 control mice and in ApoE^{-/-} mice injected with control nanobody. This focal uptake is specific as it could be blocked by an excess of unlabelled nanobody. Arrow indicates aortic arch.

Demir et al.³⁹ retrospectively reviewed 157 consecutive patients with suspected CAD who were submitted to CCTA between 2012 and 2014. They showed that the predictive models of PTP and cardiovascular risk, proposed by ESC (2013) and UK NICE (2010) guidelines, have a poor agreement and more importantly overestimate the prevalence of CAD at CCTA. Hence, more effective models are needed to better guide the appropriate use of imaging.

The high negative predictive value of CCTA could allow an effective filtering to invasive angiography in patients with low risk. Aguiar Rosa et al.⁴⁰ demonstrated that the introduction of CCTA as an additional screening test in their institution significantly increased the rate of CAD diagnosed invasively from 43 to 90% and the rate of angioplasties from 29 to 60%. Large randomized controlled trials are needed to comparatively assess the impact of imaging modalities on the diagnostic and therapeutic yield of invasive procedures.

To assess the comparative cost-effectiveness of CCTA and cardiac stress imaging (CSI) modalities, alone or in combination, to diagnose CAD, Petersen et al.⁴¹ developed a simulation model based on published literature and on the perspective of three countries: the USA, the UK, and The Netherlands (NL). Their target population was based on 60-year-old patients with 30% PTP of CAD. Despite the differences in outcome (QALYs) were small across strategies, CCTA as triage test prior to CSI was cost-effective (in the USA and NL) with CCTA + ECHO being most cost-effectiveness. Though difficult to be performed, prospective comparative cost-effectiveness studies are warranted.

Perfusion imaging by single-photon emission computed tomography (SPECT) or positron emission tomography (PET) is a robust stress imaging modality in patients with suspected or known CAD due to its well-demonstrated prognostic value. Al Mallah et al.⁴² showed that it holds true also in patients with LBBB that may cause septum perfusion defects of uncertain interpretation. In a series of 706 patients with LBBB undergoing vasodilator stress SPECT, resting and stress perfusion defects added incremental prognostic information for all-cause mortality and non-fatal myocardial infarction in a median follow-up period of 35 months.

An original application of nuclear imaging is the visualization of the calcification process in heart valves. Dweck et al.⁴³ measured active valvular calcification using PET/CT and 18F-sodium fluoride tracer (18F-NaF) in 121 volunteers with and without AS. The authors observed a significant correlation between baseline valvular 18F-NaF uptake and the progression in calcium score or echocardiographic haemodynamic measurements in a 2 years follow-up. Valvular 18F-NaF was an independent predictor of aortic valve replacement and cardiovascular death.

An exciting new application of nuclear modalities is imaging of inflammatory processes. The recognition of the vulnerable plaque is the holy grail of vascular imaging research. Vascular cell adhesion molecule-1 (VCAM-1) is expressed in inflammatory atherosclerotic lesions and is a potential target for molecular imaging of vulnerable plaques. Bala et al.⁴⁴ demonstrated that mouse/human cross-reactive anti-VCAM-1 nanobodies (Nb), radiolabelled with 18F, specifically bind with VCAM-1-positive isolated cells (Figure 6). They also showed that atherosclerotic lesions in the aortic arch of ApoE^{-/-} mice injected with 18F-anti-VCAM-1 Nb could be successfully identified using μ PET/CT imaging. Whether successfully transferred to

humans, this approach may represent an attractive tool for imaging vulnerable atherosclerotic plaques in patients.

Imaging the inflammatory process elicited in the myocardium after acute ischaemic injury is another prospectively important goal. Tierens et al.⁴⁵ used pinhole-SPECT/CT and 99mTc-labelled nanobodies targeting the macrophage mannose receptor (MMR Nb) to image M2-mediated inflammation in a myocardial ischaemia/reperfusion rat model. They demonstrated significant retention of 99mTc-Nbs in the infarcted myocardium where immunofluorescent staining confirmed the presence of MMR. These results may open new opportunities to follow the impact of various treatment strategies on inflammation modulation in acute ischaemic heart disease.

Conflict of interest: none declared.

References

- Baum P, Stoebe S, Pfeiffer D, Hagendorff H. Deformation imaging in patients with left bundle branch block: are there differences between ischemic and non-ischemic origin? *Eur Heart J Cardiovasc Imaging* 2014;**15**(Suppl. 2):ii109–36.
- Szulik M, Tillekaerts M, Vangeel V, Ganame J, Willems R, Lenarczyk R et al. Assessment of apical rocking: a new, integrative approach for selection of candidates for cardiac resynchronization therapy. *Eur J Echocardiogr* 2010;**11**:863–9.
- Mada RO, Lysyansky P, Duchenne J, Winter S, Fehske W, Stankovic I et al. New automatic tools to select candidates for cardiac resynchronization therapy. *Eur Heart J Cardiovasc Imaging* 2014;**15**(Suppl. 2):ii235–64.
- Hasselberg NE, Haugaa KH, Brunet Bernard A, Kongsgård E, Donal E, Edvardsen T. Reverse remodeling is more dependent on improvement of longitudinal function than circumferential function in cardiac resynchronization therapy. *Eur Heart J Cardiovasc Imaging* 2013;**14**(Suppl. 2):ii20–48.
- Blazquez Bermejo Z, Caro Codon J, Lopez Fernandez T, Valbuena S, Mori Junco R, Ponz De Antonio I et al. Early detection of cardiotoxicity using myocardial deformation imaging in GECAME study. *Eur Heart J Cardiovasc Imaging* 2014;**15**(Suppl. 2):ii109–36.
- Reant P, Mirabel M, Dickie S, Rosmini S, Demetrescu C, Tome-Esteban M et al. Global longitudinal strain predicts cardiovascular death in hypertrophic cardiomyopathy. *Eur Heart J Cardiovasc Imaging* 2014;**15**(Suppl. 2):ii161–4.
- Ternacle J, Bodez D, Guellich A, Rappeneau S, Dubois-Randé JL, Guendouz S et al. Causes and consequences of longitudinal left ventricle dysfunction assessed by 2d-strain echocardiography in patients with cardiac amyloidosis. *Eur Heart J Cardiovasc Imaging* 2014;**15**(Suppl. 2):ii165–7.
- Saura Espin D, Caballero Jimenez L, Oliva Sandoval MJ, Gonzalez Carrillo J, Espinosa Garcia MD, Garcia Navarro M et al. Aortic stenosis: prognostic value of planimetric anatomical valvular area as measured by 3D-TEE. *Eur Heart J Cardiovasc Imaging* 2014;**15**(Suppl. 2):ii65–7.
- Scherzer S, Geroldinger AG, Krenn L, Roth C, Gangl C, Maurer G et al. Biomarker NT-proBNP – a predictor of outcome in transfemoral aortic valve implantation? *Eur Heart J Cardiovasc Imaging* 2014;**15**(Suppl. 2):ii82–108.
- Kramer B, Hermann S, Liu D, Hu K, Ertl G, Weidemann F. Fundamental differences in disease progression, functional and clinical outcome in patients with low-gradient and high-gradient aortic valve stenosis. *Eur Heart J Cardiovasc Imaging* 2014;**15**(Suppl. 2):ii109–36.
- Galli E, Guirette Y, Auffret V, Daudin M, Fournet M, Mabo P et al. Left atrial systolic function impairment and prognosis in severe aortic stenosis. *Eur Heart J Cardiovasc Imaging* 2014;**15**(Suppl. 2):ii82–108.
- Galli E, Oger E, Guirette Y, Daudin M, Fournet M, Donal E. Risk stratification in severe aortic stenosis: the importance of ventriculo-arterial interplay. *Eur Heart J Cardiovasc Imaging* 2014;**15**(Suppl. 2):ii196–223.
- Bandera F, Generati G, Pellegrino M, Labate V, Alfonzetti E, Guazzi M. Impact of dynamic Mitral Regurgitation on functional capacity in heart failure patients. *Eur Heart J Cardiovasc Imaging* 2014;**15**(Suppl. 2):ii60–2.
- Pradel S, Mohty D, Magne J, Darodes N, Lavergne D, Damy T et al. Prevalence and prognostic significance of left-sided valvular thickening in patients with systemic light-chain amyloidosis. *Eur Heart J Cardiovasc Imaging* 2014;**15**(Suppl. 2):ii235–64.
- Mueller H, Reverdin S, Ehret G, Conti L, Dos Santos S. Measurement of left and right atrial volume: comparison of different semi-automatic algorithms of real-time 3D echocardiography. *Eur Heart J Cardiovasc Imaging* 2014;**15**(Suppl. 2):ii192.
- Luo XX, Fang F, Lee APW, Shang Q, Yu CM. Multidirectional left ventricular performance detected with three-dimensional echocardiography in patients with chronic right ventricular pacing. *Eur Heart J Cardiovasc Imaging* 2014;**15**(Suppl. 2):ii48.
- Dreyfus J, Durand-Viel G, Cimadevilla C, Brochet E, Vahanian A, Messika-Zeitoun D. A Assessment of tricuspid annulus shape and orientation using three-dimensional

- transesophageal echocardiography. *Eur Heart J Cardiovasc Imaging* 2014;**15**(Suppl. 2): ii65.
18. Sotaquirá M, Pepi M, Tamborini G, Caiani EG. Segmentation and quantification of the anatomic regurgitant orifice from transesophageal 3D echo images in patients with mitral regurgitation. *Eur Heart J Cardiovasc Imaging Abstracts Supplement* 2014; **15**(Suppl. 2):iii191.
 19. Miglioranza MH, Muraru D, Cavalli G, Addetia K, Cucchini Q, Mihaila S et al. Three-dimensional tricuspid annulus surface area is a better predictor of functional tricuspid regurgitation severity than conventional 2D-echocardiography diameters. *Eur Heart J Cardiovasc Imaging* 2014;**15**(Suppl. 2):ii180.
 20. Meyer CG, Altiok E, Al Ateah G, Lehrke M, Becker M, Lotfi S et al. 3D transthoracic echocardiography vs. Cardiac Magnetic Resonance strain analysis for the evaluation of apical wall motion after transcatheter aortic valve replacement (TAVI). *Eur Heart J Cardiovasc Imaging* 2014;**15**(Suppl. 2):ii105.
 21. Rotzak R, Aharonovich A, Geva Y, Rozenman Y. The imaging of patent foramen ovale using contrast real time three dimensional echocardiography. *Eur Heart J Cardiovasc Imaging* 2014;**15**(Suppl. 2):ii21.
 22. Goebel B, Hamadanchi A, Schmidt-Winter C, Otto S, Jung C, Figulla HR et al. Interventional left atrial appendage occlusion: added value of 3D transesophageal echocardiography for orifice sizing. *Eur Heart J Cardiovasc Imaging* 2014;**15**(Suppl. 2):ii20.
 23. Boniotti C, Carminati MC, Fusini L, Andreini D, Pontone G, Pepi M et al. Fully automated 3D left ventricular myocardial scar detection for MRI-LGE images based on Gaussian mixture model. *Eur Heart J Cardiovasc Imaging* 2014;**15**(Suppl. 2):ii118.
 24. Bergler-Klein J, Geier C, Maurer G, Gyongyosi M. Cardiotoxic effects of different anthracyclines compared to liposomal doxorubicin in an experimental study with echocardiography and magnetic resonance imaging. *Eur Heart J Cardiovasc Imaging* 2014;**15**(Suppl. 2):ii183.
 25. Maceira Gonzalez AM, Iguar B, Cosin-Sales J, Diago JL, Aguiar J, Ruvira J. Incidental non-cardiac findings on cardiac magnetic resonance. *Eur Heart J Cardiovasc Imaging* 2014;**15**(Suppl. 2):ii233.
 26. Van De Heyning CM, Magne J, Pierard LA, Bruyere PJ, Davin L, De Maeyer C et al. Prognostic value of late gadolinium enhancement assessed by cardiovascular magnetic resonance in primary mitral regurgitation. *Eur Heart J Cardiovasc Imaging* 2014;**15**(Suppl. 2):ii73.
 27. Cruz I, Dymarkowski S, Bogaert J. Value of cardiovascular magnetic resonance in patients with suspected inflammatory pericarditis. *Eur Heart J Cardiovasc Imaging* 2014;**15**(Suppl. 2):ii58.
 28. Bertella E, Petulla M, Baggiano A, Mushtaq S, Russo E, Gripari P et al. Cardiac computed tomography versus cardiac magnetic resonance for characterization of left atrium anatomy before radiofrequency catheter ablation of atrial fibrillation. *Eur Heart J Cardiovasc Imaging* 2014;**15**(Suppl. 2):ii83.
 29. Zegri Reiriz I, Alcolado A, Mendez C, Sanchez MJ, Gomez Y, Climent V et al. Left atrial volume determined by CMR predicts atrial fibrillation and adverse events in hypertrophic cardiomyopathy patients in sinus rhythm. *Eur Heart J Cardiovasc Imaging* 2014; **15**(Suppl. 2):ii162–163.
 30. Suhai FI, Toth A, Kecskes K, Czibalmos CS, Csecs I, Maurovich-Horvat P et al. The role of MRI in the differentiation of athlete's heart from Hypertrophic Cardiomyopathy. *Eur Heart J Cardiovasc Imaging* 2014;**15**(Suppl. 2):ii198.
 31. Nyktari E, Bilal S, Ali SA, Izgi C, Prasad SK. Prognostic value of myocardial viability by GE-CMR in patients with chronic ischaemic myocardial dysfunction: impact of delayed revascularization therapy. *Eur Heart J Cardiovasc Imaging* 2014;**15**(Suppl. 2):ii34.
 32. Fabregat Andres O, Estornell-Erill J, Ridocci-Soriano F, De La Espriella R, Albiach-Montanana C, Trejo-Velasco B et al. Prognostic value of pulmonary vascular resistances estimated by Cardiac Magnetic Resonance in systolic failure irrespective of etiology and presence of late gadolinium enhancement. *Eur Heart J Cardiovasc Imaging* 2014;**15**(Suppl. 2):ii209.
 33. Voilliot D, Odille FO, Mandry DM, Huttin OH, Andronache MA, Marie PY et al. Prediction of the onset of ventricular tachycardia in post-infarct patients with low left ventricular ejection fraction: usefulness of myocardial scar assessment by cardiac magnetic resonance imaging. *Eur Heart J Cardiovasc Imaging* 2014;**15**(Suppl. 2):ii152.
 34. Timoteo AT, Moura Branco L, Ramos R, Aguiar Rosa S, Agapito A, Sousa L et al. Usefulness of right ventricular and right atrial two-dimensional speckle tracking to predict arrhythmic events in adult patients with repaired tetralogy of Fallot. *Eur Heart J Cardiovasc Imaging* 2014;**15**(Suppl. 2):ii52.
 35. West C, Garcia-Aranda Dominguez B, Alonso-Gonzalez R, Li W, Uebing A. Echocardiographic assessment of the Melody percutaneous pulmonary valve system. *Eur Heart J Cardiovasc Imaging* 2014;**15**(Suppl. 2):ii78.
 36. Kutty S, Li L, Danford D, Houle H, Xiao Y, Pedrizzetti G et al. Rotation intensity and energy dissipation of right ventricular flow in tetralogy of fallot using echo contrast particle imaging velocimetry. *Eur Heart J Cardiovasc Imaging* 2014;**15**(Suppl. 2):ii52.
 37. Karsenty C, Hadeed K, Hascoet S, Amadiou R, Dulac Y, Acar P. 3D transthoracic echocardiography to assess Ventricular Septal Defect anatomy and severity. *Eur Heart J Cardiovasc Imaging* 2014;**15**(Suppl. 2):ii53.
 38. Cantinotti M, Assanta N, Crocetti M, Marotta M, Scalese M, Molinaro S et al. Pediatric echocardiographic nomograms for chamber diameters and area. *Eur Heart J Cardiovasc Imaging* 2014;**15**(Suppl. 2):ii80.
 39. Demir OM, Dobson P, Khan J, Shaw A, Papanichael ND, Alfakih K. Discrepancies between ESC and UK NICE guidance for patients with suspected coronary artery disease in subjects undergoing CT Coronary angiograms: Evaluation of the pre-test probability risk scores. *Eur Heart J Cardiovasc Imaging* 2014;**15**(Suppl. 2): ii443.
 40. Aguiar Rosa S, Ramos R, Marques H, Portugal G, Pereira Da Silva T, Rio P et al. Diagnostic and therapeutic profitability of isolated invasive coronary angiography vs guided by computed tomography angiography in patients with low/intermediate cardiovascular risk. *Eur Heart J Cardiovasc Imaging* 2014;**15**(Suppl. 2):ii263–4.
 41. Petersen SE, Genders TSS, Pugliese F, Dastidar AG, Fleischmann KE, Nieman K et al. Coronary CT angiography vs. cardiac stress imaging in the diagnostic work-up of patients with stable chest pain: comparative effectiveness and costs. *Eur Heart J Cardiovasc Imaging* 2014;**15**(Suppl. 2):ii151.
 42. Al-Mallah M, Qureshi W, Chhattahij. Incremental prognostic value of SPECT myocardial perfusion imaging in patients with left bundle branch block. *Eur Heart J Cardiovasc Imaging* 2014;**15**(Suppl. 2):ii442–3.
 43. Dweck M, Jenkins WSA, Shah AS, Vesey A, Pringle M, Chin CWL et al. 18F-NaF PET predicts disease progression in aortic stenosis. *Eur Heart J Cardiovasc Imaging* 2014; **15**(Suppl. 2):ii63.
 44. Bala G, Blykers A, Xavier C, Gillis K, Tierens S, Descamps B et al. Molecular imaging of inflamed atherosclerotic plaque with 18F-anti-VCAM-1 nanobody and PET/CT. *Eur Heart J Cardiovasc Imaging* 2014;**15**(Suppl. 2):ii55.
 45. Tierens S, Remory I, Bala G, Gillis K, Hermot S, Droogmans S et al. In vivo quantification of the longitudinal expression profile of the macrophage mannose receptor after myocardial ischemia reperfusion injury in rats. *Eur Heart J Cardiovasc Imaging* 2014;**15**(Suppl. 2):ii263.